energies

MDPI

Article

Optimization under Uncertainty to Reduce the Cost of Energy for Parabolic Trough Solar Power Plants for Different Weather Conditions

Adarsh Vaderobli [1], Dev Parikh [2] and Urmila Diwekar [1,2,*,†]

[1] Center for Uncertain Systems: Tools for Optimization & Management, Vishwamitra Research Institute, Crystal Lake, IL 60012, USA; adarsh.vaderobli@gmail.com
[2] Department of Industrial Engineering, The University of Illinois at Chicago, Chicago, IL 60607, USA; devparikh7@gmail.com
* Correspondence: urmila@vri-custom.org
† We have created a repository which includes data, manuals, and code. For information, please contact the author at urmila@vri-custom.org.

Received: 24 April 2020; Accepted: 15 June 2020; Published: 17 June 2020

Abstract: Renewable energy use can mitigate the effects of climate change. Solar energy is amongst the cleanest and most readily available renewable energy sources. However, issues of cost and uncertainty associated with solar energy need to be addressed to make it a major source of energy. These uncertainties are different for different locations. In this work, we considered four different locations in the United States of America (Northeast, Northwest, Southeast, Southwest). The weather and cost uncertainties of these locations are included in the formulation, making the problem an optimization-under-uncertainty problem. We used the novel Better Optimization of Nonlinear Uncertain Systems (BONUS) algorithm to solve these problems. The performance and economic models provided by the System Advisory Model (SAM) system from NREL were used for this optimization. Since this is a black-box model, this adds difficulty for optimization and optimization under uncertainty. The objective function and constraints in stochastic optimization (stochastic programming) problems are probabilistic functionals. The generalized treatment of such problems is to use a two-loop computationally intensive procedure, with an inner loop representing probabilistic or stochastic models or scenarios instead of the deterministic model, inside the optimization loop. BONUS circumvents the inner sampling loop, thereby reducing the computational intensity significantly. BONUS can be used for black-box models. The results show that, using the BONUS algorithm, we get 41%–47% of savings on the expected value of the Levelized Cost of Electricity (LCOE) for Parabolic Trough Solar Power Plants. The expected LCOE in New York is 57.42%, in Jacksonville is 38.52%, and in San Diego is 17.57% more than in Las Vegas. This difference is due to the differences in weather and weather uncertainties at these locations.

Keywords: solar energy; BONUS algorithm; weather uncertainties; stochastic optimization

1. Introduction

The energy crisis and climate change are two different terms but are closely related. The need for energy is rising by the day due to the increase in demand in developing countries like India and China. At the same time, the effects of using fossil fuels for producing energy are increasingly evident. The global average temperature has increased by 0.76 °C (0.57 °C to 0.95 °C) between 1850 to 1899 and 2001 to 2005, and the warming trend has increased significantly over the last 50 years. Sea levels are rising at an alarming rate, and deserts are expanding in the subtropics. These are just some of the glaringly obvious consequences of this increase in greenhouse gas emissions over the years. The main

contributors to this increase are fossil fuels. The solution to this is using alternative, less harmful, and sustainable energy sources.

The use of renewable energy sources has been on the rise in the last decade. Although efforts are being made to increase the use of these sources, renewable energy still accounted for only 11% of total energy generation in the United States in 2017, and solar power accounts for less than 1.3% of the electricity generated. This small percentage of solar power in the energy mix is due to the cost of solar power plants and their performance in the face of weather uncertainties. This paper tries to address the problem of minimizing the cost of electricity by solar power in the face of uncertainties.

1.1. Solar Technologies

There are two primary solar energy technologies. These are photovoltaics (PV) and concentrating solar power (CSP). PV directly converts light into electricity. CSP utilizes heat from the Sun (thermal energy) to drive utility-scale electric turbines. CSP systems are widely used for large-scale power generation and are the focus of current work. CSP technologies are the parabolic trough, linear Fresnel reflector, power tower, and dish/engine systems. In this work, we consider parabolic trough technology, which is traditionally employed in a large-scale power plant. In concentrating solar power systems, direct normal solar radiation is collected and converted to thermal energy that generates electricity by running a power block. In a parabolic trough system, trough-shaped solar field collectors are used to collect heat from the Sun. Each collector uses mirrors and receivers with supporting structures that can withstand winds. Each receiver consists of a metal tube coated selectively black with low emissivity and a vacuum around the tube inside a tubular glass. The heat is transported from the solar field by a heat transfer fluid (HTF) using a heat exchanger to the power block (also called power cycle) and other components of the system. The power block consists of a turbine that converts heat energy to electric energy. When there is insufficient solar energy to reach the rated capacity, the optional fossil-fuel backup system delivers supplemental heat to the HTF.

1.2. Role of Optimization and Uncertainties in Solar Power Systems

The abundance of solar radiation, its renewable nature, its scalability, its ease of application, and the recent boost towards green energy make solar thermal power plants an enticing opportunity for business owners. Solar power plants convert high-temperature high-energy solar radiation into thermal energy using concentrating systems. Direct normal irradiance is a metric characterizing the annual sum of direct solar radiation for a specific location. The best location for setting up a CSP plant is usually one with higher direct normal irradiance, typically arid desert areas or semi-arid areas [1]. However, it is useful to have a local solar power plant.

The comparative difference between non-renewable energy sources and solar thermal energy of considerably lower wattage has a higher cost of electricity. Optimization thus provides a window to increase efficiency and reduce the cost of electricity. Traditionally, solar thermal power plants occupy a larger area of land to increase the incident solar radiation for better energy generation. Other factors, such as the cost of equipment, maintenance costs, labor, and equivalent electricity production pose a roadblock for this technology.

A feasibility study carried out by Poullikkas et al. (2010) in the Mediterranean region found that size and capital cost are critical factors affecting the economic viability of solar power plants in the presence of feed-in incentives. [2] In a separate study, Poullikkas et al. tried to optimize technical and economic aspects of a parabolic CSP plant with a single parabolic trough without thermal storage options. They observed that CSP plants of 50 MWe capacity with thermal storage provided lower system electric unit cost in comparison to CSP plants with 100 MWe or larger capacity without thermal storage options [3].

Solar multiple is the unit used to express the solar field area against the power cycle capacity and is generally used to optimize the field area for a given power cycle capacity and/or site location. Montes et al. used solar multiple as a performance indicator for a parabolic trough solar power plant

with direct steam generation coupled with thermal storage and observed that solar multiple directly affected the levelized cost of electricity and a high solar multiple reduced the annual fossil fuel consumption [4].

In a subsequent study, Montes et al. optimized the solar multiple for a solar-only power plant of 50 MWe capacity without any hybridization or thermal storage capabilities. For their case, they considered five parabolic-trough-type plants with varying field sizes while other input parameters remain constant and calculated the solar multiple for the minimum levelized cost of electricity (LCOE) for each plant. Their results show that the optimum solar multiple is also dependent on design point conditions, power block parameters, and power cycle apart from the site location and solar field size. This study concludes that solar field size plays a big role in optimizing electricity generation, that lowering the cost of electricity for a larger-than-optimum field results in increased cost through energy loss, and that a smaller field serves just a part-load power block condition [5].

Desai et al. analyzed the effect of design parameters such as turbine inlet pressure and temperature, design radiation, size of the plant, and changes in the Rankine cycle on the levelized cost of electricity as well as the thermo-economic analysis of CSP plants. Their results indicate that an increase in the inlet temperature and plant size and a modified Rankine cycle decrease the levelized cost of electricity while improving the overall operational efficiency of the plant [6].

A solar thermal power plant converts incident solar energy into thermal energy and for electricity generation. Conventional parabolic trough types of solar thermal power plants used synthetic oil as a heat transfer fluid for transferring thermal energy to the Rankine cycle turbine. Odeh et al. evaluated a direct steam generation solar collector for its thermal performance in a parabolic trough solar plant and showed that the thermal losses were lesser than those in a synthetic-oil-type CSP [7]. Post et al. tried to optimize the heat-to-energy conversion methods using thermionic generation technology, which directly converts heat to electricity at high temperatures by applying solid-state conversion techniques. Their results suggest that thermionics shows good scope as a high-temperature topping cycle application in a CSP plant but currently needs more research to be used in power generation [8].

Another study by Bishoyi et al. simulated a CSP plant to evaluate the design and thermal characteristics of a 100-MW plant with 6 h thermal storage capacity based in Udaipur, India. HITEC solar salt is used as the HTF due to its high heat-carrying capacity, and their results verify the design to show good thermal performance [9]. Molten salt as an HTF in a parabolic-trough-type plant can be used to reduce the LCOE, as shown by Ruegamer et al. The use of molten salts as HTFs, combined with enhanced collector technology and higher power block efficiencies, show that the LCOE can be reduced greatly [10]. A study carried out by Lenert et al. optimized the solar radiation receivers by using nanoparticles with Therminol VP-1 as the HTF to improve solar–thermal energy conversion and reduce energy losses [11].

Sioshansi and Denholm analyzed the effect of thermal energy storage on the value of CSP plants through an increase in the utilization of thermal energy from the solar field. However, this is highly dependent on the plant location due to the capital costs associated with it [12]. [Most solar thermal power plants in the recent past have thermal storage to increase electricity generation and the plant capacity. Avila Marin et al. tried to find the best combination of thermal storage and turbine power to further reduce the levelized cost of electricity. The same study also compared the technology by comparing plants that used direct steam generation (DSG) and molten nitrate salts (MNS) without thermal storage capabilities and suggested areas for development of components by a cost analysis of the same plants for large-scale electricity generation. Their results show that the combination of MNS technology with high thermal storage capacity resulted in a low turbine power capacity, while DSG technology coupled with low thermal storage capacity could produce high values for turbine power. Separately, without any thermal storage, DSG was more promising than MNS to optimize the levelized cost of electricity [13].

Commercialization of CSP-type power plants faces problems in providing an economically feasible alternative to traditional power plants, and one way of tackling this issue is by optimizing the power

block for better efficiency. Mittelman et al. suggested a modified power block, adding a bottoming Kalina cycle combined with a back-pressure turbine using ammonia water as a working fluid for a 50-MW power plant, and the modified power block showed a reduction in the cost of electricity [14]. Sait et al. suggested structural design changes in the power block, including linear Fresnel collectors and multi-pass heat exchangers to reduce the cost of CSP [15].

Linear-Fresnel-type solar power plants are another type of solar power plant which uses concentrated energy and transfers this energy to a heat transfer fluid for subsequent electricity generation. Linear Fresnel reflectors with direct steam generation options are a cheaper alternative to parabolic trough systems CSP but they have certain drawbacks, such as saturated steam, which require such plants to have higher aperture area requirements. Desai et al. try to integrate both the systems to propose a composite solar thermal plant to suggest an optimal functioning solar thermal plant with a reduction in cost in comparison to both CSP- and LFR-type plants [16].

In research conducted by Boukelia et al., optimization of a parabolic trough solar thermal power plant was carried out based on an artificial neural network algorithm. Their research is based on optimizing five parameters: design parameters such as ambient temperature, direct solar radiation, row spacing between parallel collectors, the number of storage hours (TES capacity), and the solar multiple. These parameters affect the physical behavior of the CSP type plant greatly. By finding an optimized combination of all these input parameters using the ANN algorithm, they were able to minimize the LCOE and suggested an optimum system design [17]. Cabello et al. tried a similar approach using a genetic algorithm for optimization of annual profit from a parabolic trough solar plant by setting input parameters as the collector surface, thermal storage size and auxiliary system power capacity [18].

A recent review of the economic assessment of CSPs [19] presents several articles and identifies two dominant methodologies for the calculation of LCOE. It argues that, while a small subset of studies considered the time-varying meteorological and electricity market, it is an important factor and should not be neglected in policymaking.

Although uncertainty is inherent in solar power systems, only recently it has received some attention in the literature. Munoz et al. [20] studied the effect of uncertainties in solar radiation and thermal demand on the reliability of solar thermal systems. Jain et al. [21] explored the feasibility of developing a 100-MW solar thermal power plant with different degrees of thermal energy storage at Jodhpur, Rajasthan, India. The feasibility was assessed considering different scenarios of varying solar multiples and thermal energy storage. It has been concluded that uncertainties significantly affect the cost of electricity. Meybodi and Beath [22] considered effects of weather as well as cost uncertainties on various solar thermal plants in Australia. They found that the LCOE is highly dependent on the size as well as the site location of the plant. Hanel and Escober [23] studied effects of uncertainties in solar energy resource assessment on the cost of energy in Chile. The methodology for stochastic modeling to incorporate uncertainty in solar thermal power plant evaluations is presented by a study from Sandia National Laboratories [24]. Scheduling, planning, and bidding strategy in the face of uncertainties is the focus of [25–29].

From the literature survey presented in this section, it is obvious that, currently, there is no study that presents the optimization of a solar thermal power plant in the face of weather and cost uncertainties. This is the focus of the current endeavor.

1.3. Motivation and Problem Formulation

None of the optimization studies in the present literature considered uncertainties in weather and/or cost, which is inherent in solar thermal systems. The motivation behind this paper was to carry out multivariable optimization of a solar power system in the face of uncertainties. In this work, we used a new algorithmic framework based on the Better Optimization of Uncertain Systems (BONUS) algorithm proposed by Sahin and Diwekar [30] and the System Advisor Model (SAM) [31] simulation software developed by the National Renewable Energy Laboratory (NREL). We reduced

the expected value of the levelized cost of energy under power constraints in parabolic trough solar power plants in the face of uncertainties.

We use SAM to simulate the technical and financial parameters of the power plant, which helped us in identifying the decision variables and uncertain variables involved in our problem. We then used the BONUS algorithm framework to optimize these decision variables, including uncertainties in weather and cost, to get our lowest-cost objective function. We selected four different locations with different weather conditions for the parabolic trough plant to be situated at.

2. The System Advisory Model and Problem Definition

The System Advisor Model (SAM) [31] is a simulation model developed at NREL with help from Sandia National Laboratories, the University of Wisconsin, and other organizations. SAM includes performance and cost models that can simulate grid-connected power projects based on different types of renewable sources of energy. This is a highly useful tool for people working in the renewable energy sector. SAM uses information about technical parameters, like the type of equipment, the design of the equipment, and the configuration of the system, as inputs to make performance predictions, which then enable it to make cost-of-energy estimates using financial variables such as installation costs, labor costs, operation and maintenance costs. The performance models can run hourly simulations to calculate the power system's electrical output. Yearly electricity output and the cost of electricity are then calculated from this hourly output. The different renewable energy sources that SAM can handle include photovoltaic systems, concentrating solar power systems, solar water heating, wind power, geothermal, and biomass power. The financial models in SAM can either represent a residential or commercial project that can buy and sell electricity from and to the grid or power purchase agreement.

SAM uses weather data; location information, such as the area coordinates, wind speed, average temperature, and elevation above sea level, is stored in weather files. The weather data elements differ for each performance model. For example, for solar technologies, the weather file consists of data elements, such as global horizontal, direct normal and diffuse horizontal irradiance, used to calculate incident irradiance. It should be noted that there are measurement and model uncertainties with this parameter, as indicated in recent literature [32,33]. Meanwhile, the wind power performance model requires wind speed and temperature data at three different heights above the ground along with wind direction and atmospheric pressure data.

SAM's solar resource library for weather data includes NREL's National Solar Resource Database, Solar and Wind Energy Resource Assessment Program, ASHRAE International Weather for Energy Calculations, version 1.1, and Canadian Weather for Energy Calculations.

In this work, we used one-year data for four different regions in the USA. Thus, seasonal uncertainties are included in the problem.

3. Problem Definition and Decision Variables

The problem at hand is to minimize the expected value of the levelized cost of electricity subject to the capacity (power plant size) constraint.

$$Minimize\ E(C_E\ (x,u)) \tag{1}$$

$$Subject\ to\ Ca(x,u) = 100 \tag{2}$$

$$SAM\ model\ equations\ S(x,u) = 0 \tag{3}$$

Here, E denotes the expected value and P is the probability of satisfying the constraint. C_E denotes the LCOE of electricity and Ca the capacity of the power plant. We considered the capacity of the power plant to be 100 MW. Equation (3) represents all the black-box model equations of SAM. All these quantities are functions of the decision variables, x, and the uncertainties in weather and cost are denoted by variables, u.

The parameters for the parabolic trough physical model in SAM are divided for different sections of the plant, like the solar field, collectors, receivers, power cycle, thermal storage, and parasitic. We targeted the solar field parameters for choosing the decision variables for our problem. To determine the decision variables from all the solar field parameters, we performed a sensitivity analysis to see the effect of these parameters on the annual energy calculated by the model. The most sensitive parameters were selected for optimization. These parameters are given below.

- Solar multiple: The solar field aperture area required to generate the thermal energy needed to achieve the rated capacity. Thermal and optical losses are included in the capacity.
- Row spacing: The distance between rows of collectors in meters when the rows are placed uniformly throughout the solar field.
- Stow angle: The hour of stow collector angle. Northern latitude represents a zero stow angle and is vertical facing east, and a 90 degree angle is vertical facing west.
- Freeze protection temperature: This is the minimum temperature of the heat transfer fluid at which the freeze protection equipment is activated.
- Irradiation at design: The design point direct normal radiation value. The aperture area required to drive the power cycle at its design capacity and the design mass flowrate of the heat transfer fluid is calculated based using the value of irradiation
- Collector tilt: This is the angle from horizontal of all collectors in the field. It is assumed that all collectors are fixed at this angle. Closest to the equator, a positive value tilts the end of the array up; at the southern end, a negative value tilts it down.

Apart from weather uncertainties included in the weather data file, we considered uncertainties in the following cost parameters.

3.1. Direct Capital Costs

- Site Improvements ($/m2)—This is the cost in dollars per meter square, which includes expenses related to site preparation and other equipment that are not included in the solar field cost category.
- Solar Field ($/m2)—This is the cost of solar field area in dollars per meter square, which includes expenses related to the installation of the solar field, labor, and equipment.
- HTF System ($/m2)—These are the expenses related to the installation of the heat transfer fluid pumps and piping, labor, and equipment expressed in dollars per square meter of the solar field area.
- Storage ($/kWht)—Storage capacity cost dollars per thermal megawatt hour, which includes expenses related to the installation of the thermal storage system, equipment, and labor.
- Power Plant ($/kWe)—Cost of power block gross capacity. This includes the installation of the power block, equipment, and labor.

3.2. Indirect Capital Costs

- EPC and Owner Costs—Costs associated with design and construction. Costs of land tax and insurance rates consider federal and state income tax rates, sales tax, insurance rate, inflation rate, and real discount rate.

4. The BONUS Algorithm

In optimization, the values of decision variables are determined by optimizing the objective function and satisfying the constraints. The presence of uncertainties converts the optimization problem into a stochastic optimization problem. There is a probabilistic objective function as the expected value or variance in a stochastic optimization problem. The constraints can also be probabilistic. A generalized stochastic optimization problem [34] can then be represented as:

$$Optimize\ P_1(Z(x,u)) \tag{4}$$

$$subject\ to\ P_2(h(x,u)) = 0 \tag{5}$$

$$P_3(g(x,u) \geq 0) \tag{6}$$

where P is some form of function-derived cumulative distribution functional and u is the uncertain variable expressed in terms of probability distributions. x denotes decision variables. In our problem, the objective function is the expected value in the face of the capacity constraint.

Stochastic optimization problems can be categorized as stochastic linear programming, stochastic nonlinear programming, and stochastic mixed-integer linear and nonlinear programming problems. Our problem involves continuous decisions and nonlinear functions and hence is a stochastic nonlinear programming problem.

Figure 1 represents the general calculation sequence for these problems [35]. The inner loop finds a probabilistic representation of the objective function and constraints using the sampling loop or scenario loop. The outer optimization loop determines the decision variables. For these decision variables at each iteration, a sample set or scenario set of uncertain variables is generated, the model is run for each of these sample (scenario) points, and the value of the probabilistic objective and constraints are calculated. For nonlinear programming problems, the derivative information is also needed, which is again calculated by perturbation of each decision variable using the sampling loop or scenario loop for each perturbation.

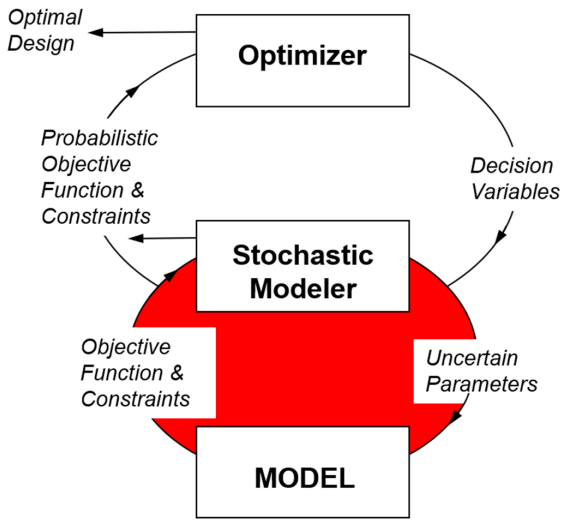

Figure 1. Pictorial representation of a stochastic optimization problem (Reproduced from Diwekar and David, 2015).

The two fundamental approaches used to solve Stochastic Nonlinear Programming (SNLP) problems include techniques that identify problem-specific structures and transform the problem into a deterministic NLP problem and problems that use decomposition techniques. For instance, chance-constrained programming [36] replaces the constraints that include uncertainty with the appropriate probabilities expressed in terms of moments, thereby transforming the problem into a deterministic optimization problem that comes under the first category. For example, the stochastic unit commitment problem in the power industry is often handled as a chance-constrained programming problem [37]. However, there are major restrictions in applying the chance-constrained formulation; for instance, the technique is only applicable to stable distribution functions, the uncertain variables should appear in the linear terms in the chance constraint, and, further, the problem needs to satisfy the general convexity conditions. Constraint correlations can create problems for chance-constrained programming. The chance-constrained information decision gap method is another way of handling uncertainty [38]. Robust optimization [39] techniques consider the worst-case scenario and also require a transformation of the problem. However, these methods are difficult to apply to black-box

systems like the one we have here. Decomposition techniques, like L-shaped decomposition [40], use stages to divide the problem. These involve master problems and subproblems. The subproblems generate bounds on the objective function for the master problem by changing decision variables, and s determines the recourse action with respect to the uncertain variables. However, these methods also require convexity conditions and/or dual-block angular structures and are only applicable to discrete probability distributions (for example, Lagrangian-based approaches and regularized decomposition technique [41] and the progressive hedging algorithm [42] used for SNLPs). These methods have limitations in terms of handling uncertain variables as the number of scenarios considered tend to be small. An alternative approach that can be used to capture uncertainty is through a sampling loop that is run for every optimization iteration for the decision variables, as shown in Figure 1. Examples of this approach include stochastic approximation methods like Dantzig's method of importance sampling [43] and the stochastic decomposition method proposed by Higel and Sen [44]. These methods generate upper and lower bounds for the approximation of the stochastic function. This is a computationally expensive procedure making these methods ineffective for even moderately complex models. The Better Optimization of Nonlinear Uncertain System (BONUS) algorithm was proposed by Sahin and Diwekar in 2004 [30] to circumvent this problem. In BONUS, the inner sampling loop with sample model runs (Figure 1) is only used for the first iteration. In this first iteration, the decision variables are assumed to have uniform distributions (between upper and lower bounds). Specified probability distributions of uncertain variables, together with the uniform distribution of decision variables, form the base distributions for analysis. The solution space of the objective function and constraints is obtained by sampling only at the base distribution at the beginning of the analysis. As the optimization proceeds, the decision variables change, and the underlying distributions for the objective function and constraints transform. A reweighing scheme is used based on the ratios of the probabilities for the current and the base distributions to find the values of the objective function and constraints. To obtain a smooth function for the probabilities, we approximate the distributions using kernel density estimation techniques. For details, please refer to Sahin and Diwekar [30] and Diwekar and David [34] Thus, there are no sampling loop and model evaluations for each optimization iteration in BONUS. Even the derivative information is calculated using reweighing. We use the efficient Hammersley sequence sampling (HSS) [45,46] for the base distributions to increase the computational efficiency further. The algorithm we have developed is essentially a sequential quadratic programming (SQP) algorithm that replaces the sampling loop and uses a reweighting scheme to estimate the objective function and gradient at each iteration. The Hessian is approximated by using a BFGS formula.

The general procedure involves the following steps. Since we need an expected value for objective function and constraint for this problem, the procedure is described in terms of expected value calculations.

1. *Off-line Computations:* Draw independently distributed samples j = 1, Nsamp for uncertain variables u and decision variables x. The distributions for the decision variables are assumed to be uniform distributions between the upper and lower bounds of the decision variables. Use these samples to generate the design prior density function $P^p(x,u)$ using Kernel Density Estimation (KDE). Evaluate the objective function Z (and the probabilistic constraint) for each sample.
2. *On-line Computations*:

    a. At each iteration, k, the decision variables x^k (in the first iteration, the initial value of the decision variables is given) define a narrow normal distribution around this point and draw samples of x^k from it. Use samples to generate the design distribution $P^d(x,u)$ using KDE. Estimate the objective function and constraint (expected value E) using the following reweighting formula.

$$V\left(x^k\right) = E(Z(x,u)) = \sum_{j=1}^{Nsamp} \omega_j^k Z\left(x^k,u\right) \tag{7}$$

where

$$\omega_j^k = \frac{P^d\left(x_j^k, u\right) / P^p\left(x_j^k, u\right)}{\sum_{jj=1}^{Nsamp} P^d\left(x_{jj}^k, u\right) / P^p\left(x_{jj}^k, u\right)}$$

and satisfy $\sum_{j=1}^{Nsamp} \omega_j^k = 1$.

b. Perturb the decision variable x^k and use the reweighting scheme to estimate $(x^k + \delta\, x^k)$. Find the gradient and KKT conditions. If KKT conditions are satisfied, terminate and go to step 2c.

c. SQP-based NLP: The Hessian approximation H^k is calculated using a gradient using BFGS formula. Compute step Δx for decision variables by solving a quadratic program (QP):

$$\min_{\Delta x} \nabla V(x^k)^T \Delta x + \Delta x^T H^k \cdot \Delta x \tag{8}$$

$$s.t.\ x^k + \Delta x \tag{9}$$

d. Decrease the step if necessary to obtain a new iterate $x^{k+1} = x^k + \alpha \Delta x$ with $\alpha \in (0, 1)$.

e. Go to step 2a.

5. Results and Discussions

For using BONUS, the first step is to generate a base sample set. We identified the six decision variables (Table 1) and 13 uncertain variables (Table 2) using SAM's physical parabolic trough model in the previous section. Overall, 2000 samples of these 19 variables are generated using HSS. Decision variables are assigned a uniform distribution with their upper and lower bounds specified. Normal distributions are assigned to the uncertain variables.

Table 1. Decision variables and their bounds.

Parameter	Lower Bound	Upper Bound
Collector Tilt	0	7
Freeze Protection Temp.	140	180
Irradiation at Design	800	1000
Row Spacing	10	20
Solar Multiple	1	3
Stow Angle	150	180

Table 2. Uncertain variables with mean, std. dev. and bounds.

Parameter	Mean (μ)	Std. dev. (σ)	Lower Value ($\mu - 3\sigma$)	Upper Value ($\mu + 3\sigma$)
HTF System Cost per meter square	60	1.65	54	66
Land Cost per acre	10,000	330	9000	11,000
Power plant cost per Kwe	1200	29.04	1080	1320
Site Improvement cost per meter square	40	0.66	36	44
Solar field cost per meter square	450	11.55	405	495
Storage system cost per kWht	75	2.31	67.5	82.5
EPC Costs % direct	11	0.495	9.9	12.1
Inflation Rate	1	0.0825	0.9	1.1
Real Discount Rate	2	0.1815	1.8	2.2
Federal income tax rate	28	0.924	25.228	30.772
Insurance rate	0.5	0.0165	0.4505	0.5495
Sales Tax	5	0.165	4.505	5.495
State Income Tax	5	0.231	4.5	5.5

After 2000 sample runs of SAM, we collected the output information, which defines the objective function and the constraint. BONUS is then used to find optimal solutions for all four different locations.

It has been found that the four stochastic nonlinear problems are non-convex. To avoid getting trapped in local solutions, we provided ten different initial values for the algorithm. These different initial values needed different iterations to get to the optimum. The version of BONUS developed in our group uses Successive Quadratic Programming (SQP) for derivative-based nonlinear optimization. Therefore, the iteration summary for each SQP run is plotted. Since this is an NLP problem, we used Karush–Kuhn–Tucker (KKT) error for the stopping criteria. The tolerance for KKT error is set to 0.001% of the objective function value. Figures 2–5 show the optimization iteration summary. The best value from all the iterations is reported in Table 3.

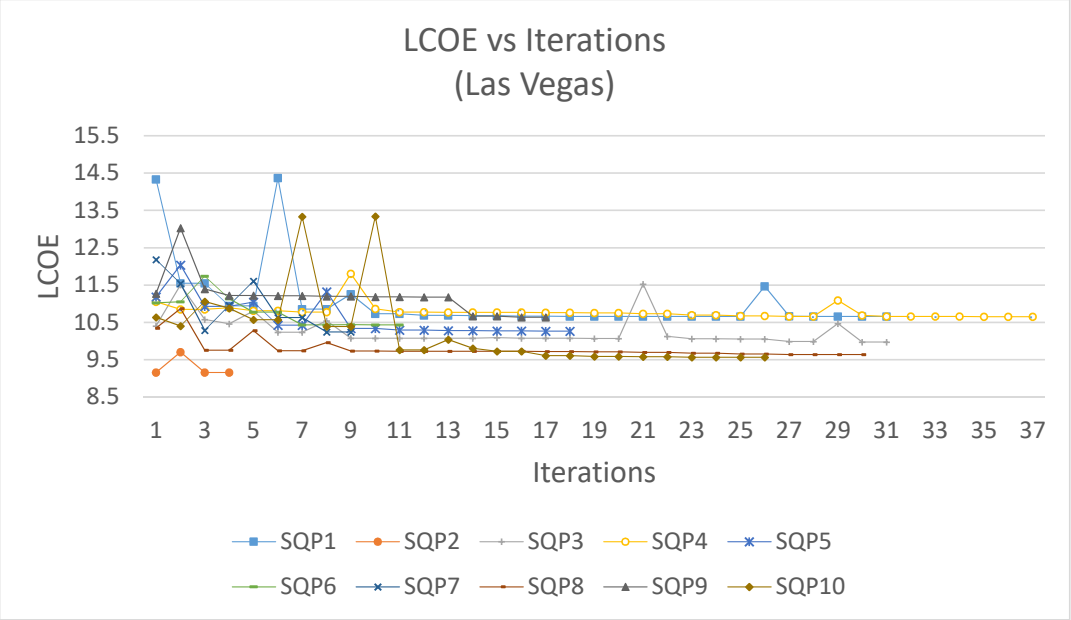

Figure 2. Optimization iteration summary for Las Vegas.

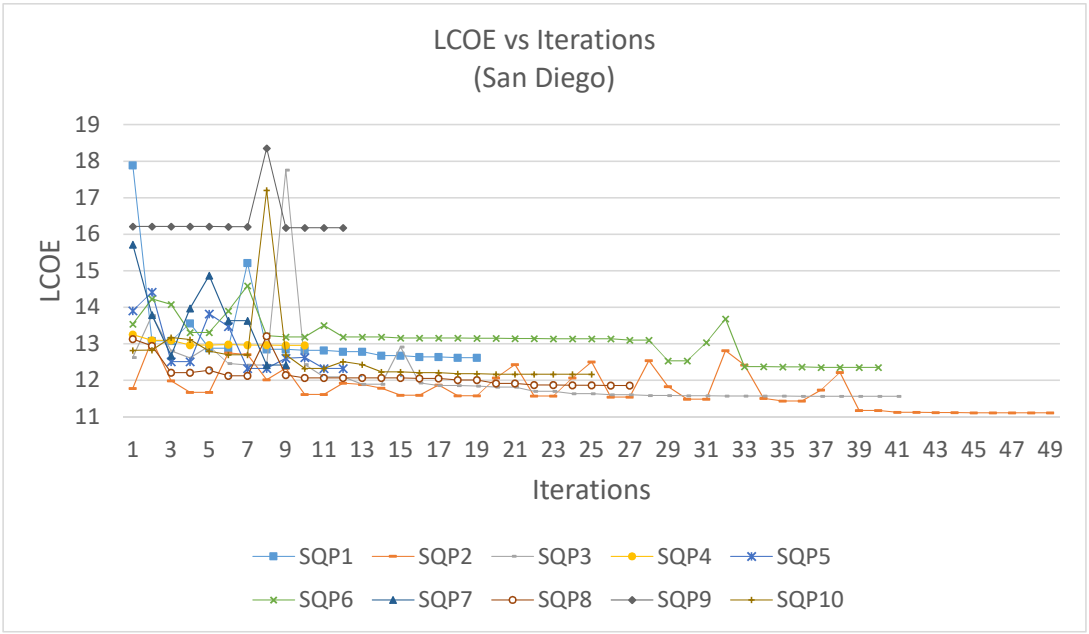

Figure 3. Optimization iteration summary for San Diego.

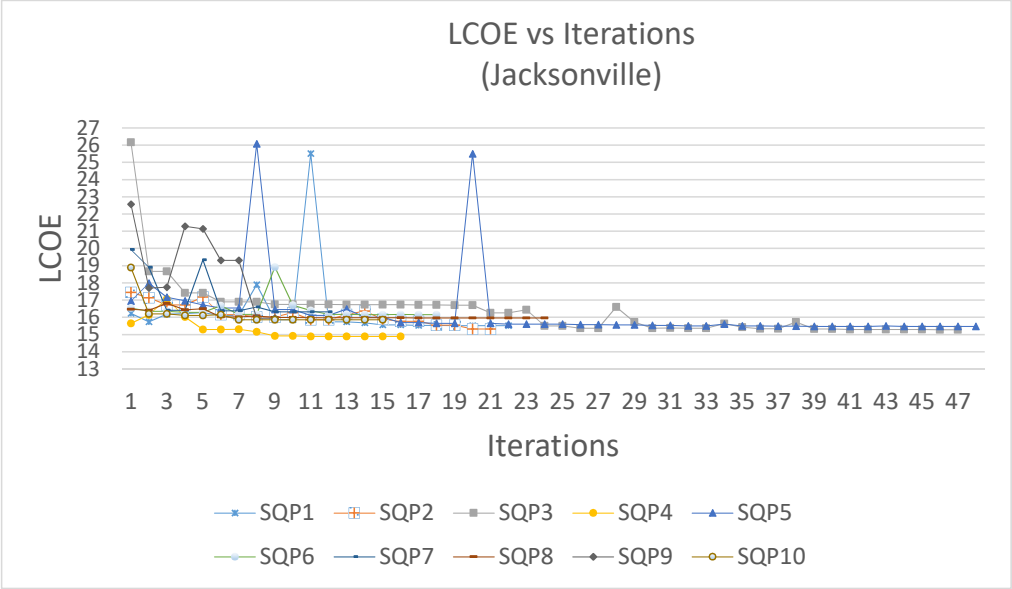

Figure 4. Optimization iteration summary for Jacksonville.

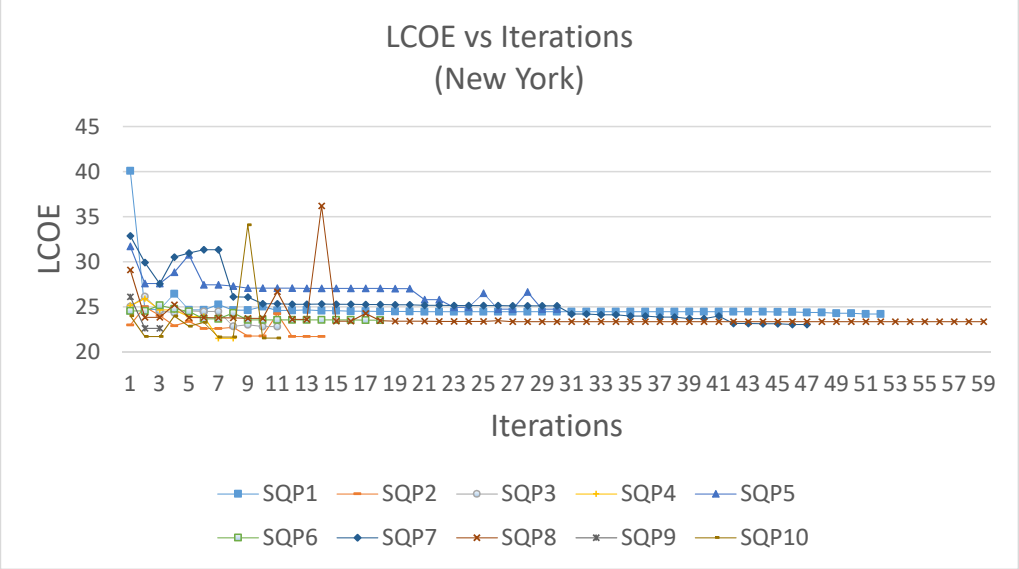

Figure 5. Optimization iteration summary for New York.

Table 3. Optimal values and cost savings for different locations with consideration of uncertainties.

Decision Variables	San Diego (Base Case)	Las Vegas (Optimal)	San Diego (Optimal)	Jacksonville (Optimal)	New York (Optimal)
Collector Tilt	0	0.97883	0.91945	1.0382	0.77559
Freeze Protection Temp	150	145	164.09	165	168.49
Irradiation @ Design	950	830	829.94	830	840.08
Row Spacing	15	17.001	17.63	16.818	15.886
Solar Multiple	2	2.2341	2.3632	2.3841	3
Stow Angle	170	162	162.58	162.01	161.9
Base Value, Deterministic, LCOE		16.91	21.18	29.98	43.22
Base case E(LCOE)		16.91	21.144	29.97	43.21
Optimal E(LCOE)		9.947	12.19	15.69	23.1
BONUS Optimal E(LCOE)		9.155	11.106	14.89	21.5
% savings		41.17682	42.34771	47.64765	46.54015
% difference bonus & actual		7.9622	8.892535	5.098789	6.926407

Since BONUS uses reweighting for approximating the value of the objective function, we carried out a full-scale stochastic simulation with 2000 samples at the optimal values to find the exact E(LCOE). The optimal values of the decision variables for different locations and their cost savings are shown in Table 3. We also carried out deterministic optimization, and the results are shown in Table 4.

Table 4. Deterministic optimization results.

Decision Variables/Optimal Cost	Las Vegas	San Diego	Jacksonville	New York
Collector tilt (deg)	0.2694	0.2694	3.995	5.6287
Freeze protection temp (°C)	154.707	154.707	170.82	157.266
Irradiation at design (W/m^2)	815.181	815.181	826.246	942.112
Row spacing (m)	19.8304	19.8304	18.8608	12.752
Solar multiple	2.8909	2.8909	1.1441	2.7076
Stow angle (deg)	177.428	177.428	3.995	157.618
Avg. LCOE (cents/kWh)	11.395	13.65	21.288	29.433
Value of Stochastic Solution(cents/kWh)	1.448	2.544	5.538	6.333

As can be seen, the table reaches different optimal values for each of the four locations. The decision variable values are also different for each location due to the weather conditions. The optimal decision variable values are different for deterministic optimization and stochastic optimization. This can be attributed to the cost and weather uncertainties. The value of the stochastic solution is the difference between the stochastic optimal cost obtained using stochastic optimization and the stochastic cost at the deterministic optimum. It has been found that the value of the stochastic solution is highest for New York. Given that New York weather changes considerably over different seasons, this is an expected result. Table 3 shows that the optimal solution with respect to the expected value of LCOE is 41 to 47.7% better than the base case. Las Vegas has the lowest cost; the expected LCOE in New York is 57.42%, in Jacksonville is 38.52% and in San Diego is 17.57% more than in Las Vegas. It has been found that, although BONUS captures the trends and hence the correct optimal values of the decision variables, it underestimates the objective function by 5 to 8.9%. This can be easily corrected by undertaking a stochastic simulation at the end of the final run, as we have done here. However, with BONUS, we save on computational time significantly, as shown below.

5.1. Computational Savings

We can compute the reduction in computational time using the following formula (here, we assume that one SAM run is approximately the same):

$$\text{Reduction in computational time} = \frac{\textbf{Difference in no. of SAM runs required}}{\textbf{Original no. of SAM runs r}} \times 100 \quad (10)$$

The total number of iterations required for optimizing the plant is 68. Since there are six decision variables and 500 sample points, the original number of SAM runs required would be $(6 + 1) \times 500 \times 68 = 238{,}000$. We simulated 2000 calculations using SAM. Hence, the difference in the number of iterations is $238{,}000 - 2000 = 236{,}000$. Therefore, the reduction in computational time is

$$\text{Reduction in computational time} = \frac{236,000}{238,000} \times 100 = 99.15966\% \quad (11)$$

5.2. Effect of Individual Decision Variables

We have investigated the effect of each variable on the objective function. Here, we only considered the deterministic objective function. For this, we use five different values of each decision variable and the rest remain constant. We run our simulations in SAM and plot the graphs of each decision variable, which are shown in Figures 6–8. The actual optimal value found is shown with a red dot. As can be seen, the optimal value is lower than the trends. This is because we are carrying out a multivariable optimization instead of a single-variable optimization. Further, uncertainties are also

affecting the optimal value, as can be seen from Table 3. The deterministic base case value is higher than the stochastic (E(LCOE)) value.

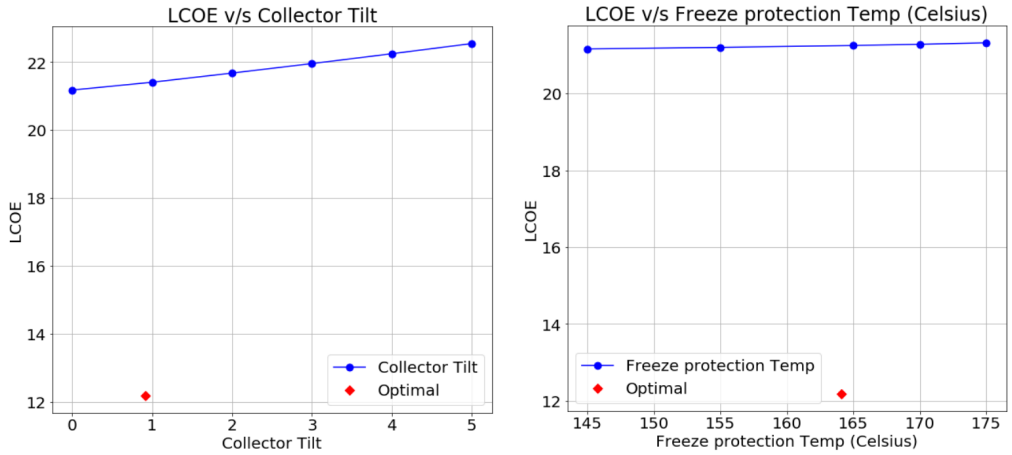

Figure 6. Effect of the decision variables collector tilt and freeze protection temperature on LCOE.

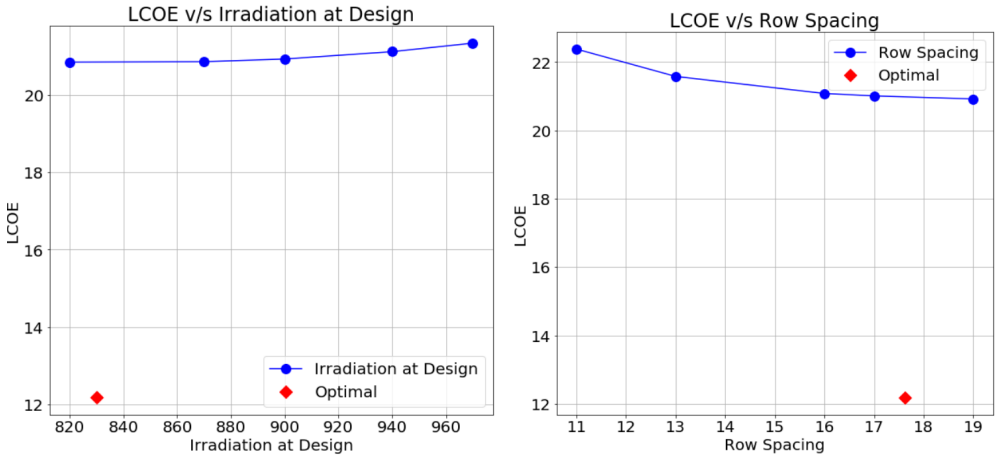

Figure 7. Effect of the decision variables irradiation and row spacing on LCOE.

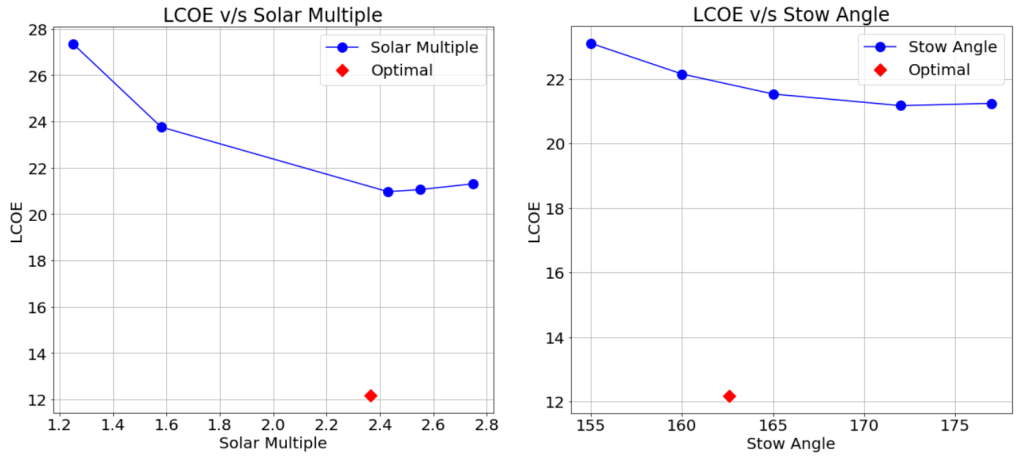

Figure 8. Effect of the decision variables solar multiple and stow angle on LCOE.

The stochastic simulation results for the base case, deterministic optimal values, and stochastic optimal values are plotted in Figures 9 and 10. We can see that the base case, deterministic optimal,

and stochastic optimal case CDFs do not cross each other, showing that the stochastic optimal case is also a robust design in the face of uncertainties.

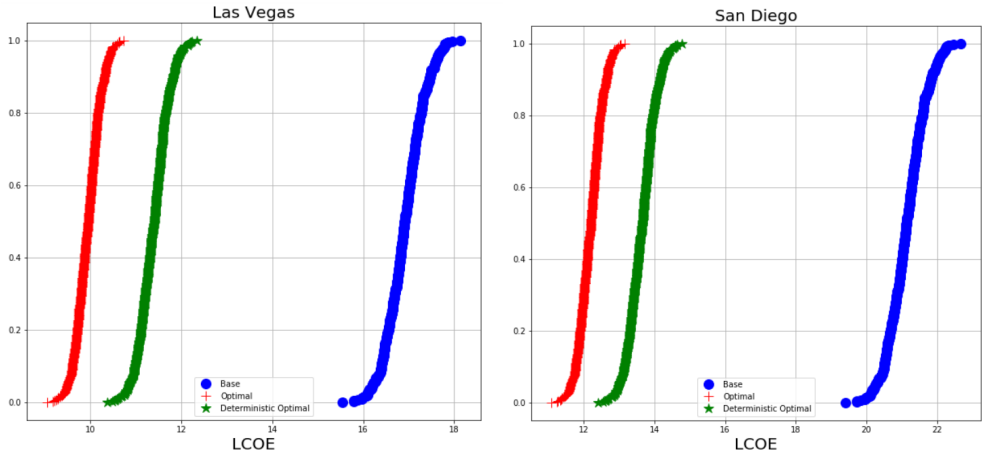

Figure 9. Comparing the CDF of LCOE at the base, deterministic optimal, and stochastic optimal for Las Vegas and San Diego.

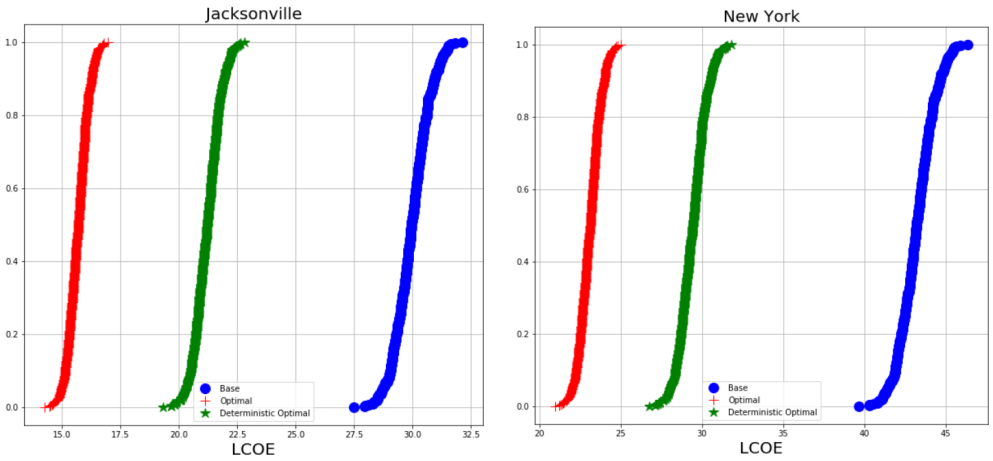

Figure 10. Comparing the CDF of LCOE at the base, deterministic optimal, and stochastic optimal for Jacksonville and New York.

6. Summary and Future Work

This work presents, for the first time, multi-variable optimization of a parabolic trough power plant in the face of uncertainties. SAM was used to model the performance and cost of the power plant. Sensitivity analysis was used to determine which decision variables to use for optimization. The BONUS algorithm provided optimal solutions for the 100-megawatt solar power plants under weather and cost uncertainties for four locations. BONUS is shown to be 98 to 99% more efficient than traditional stochastic nonlinear programming frameworks.

The US Energy Information Administration (EIA [47,48]) has predicted the levelized cost of energy for different energy sources in 2020 [43]. The estimated LCOE for solar thermal technology in 2020 is 23.97 cents/kWh, and for advanced coal technology it is 11.57 cents/kWh. The recent energy outlook [42] does not provide the cost of CSPs but provides estimates of energy cost. The energy cost is predicted to decrease because of natural gas projections. By 2050, prices will range from 9.7 cents/kWh to 11.6 cents/kWh across high and low oil and gas resource and technology cases [44]. We estimated, for the 100 MW plants, 9.95, 12.19, 15.69, and 23.1 cents/kWh for Las Vegas, San Diego, Jacksonville, and New York, respectively. Given that these estimates are calculated without including subsidies and tax incentives, the cost seems to be comparable.

Author Contributions: Conceptualization, U.D.; methodology, U.D.; software, A.V., D.P. and U.D.; validation, A.V. and D.P.; formal analysis, A.V., D.P. and U.D.; investigation, A.V., D.P. and U.D.; resources, U.D.; data curation, A.V.; writing—original draft preparation, A.V. and D.P.; writing—review and editing, U.D.; visualization, A.V.; supervision, U.D.; project administration, U.D.; funding acquisition, U.D. All authors have read and agreed to the published version of the manuscript.

Funding: The work is partially funded by a grant from Devon Energy.

Conflicts of Interest: The authors declare no conflict of interest.

References

1. Fernández-García, A.; Zarza, E.; Valenzuela, L.; Pérez, M. Parabolic-trough solar collectors and their applications. *Renew. Sustain. Energy Rev.* **2010**, *14*, 1695–1721. [CrossRef]
2. Poullikkas, A.; Kourtis, G.; Hadjipaschalis, I. Parametric analysis for the installation of solar dish technologies in Mediterranean regions. *Renew. Sustain. Energy Rev.* **2010**, *14*, 2772–2783. [CrossRef]
3. Poullikkas, A.; Hadjipaschalis, I.; Kourtis, G. The cost of integration of parabolic trough CSP plants in isolated Mediterranean power systems. *Renew. Sustain. Energy Rev.* **2010**, *14*, 1469–1476. [CrossRef]
4. Montes, M.J.; Abánades, A.; Martínez-Val, J.M. Performance of a direct steam generation solar thermal power plant for electricity production as a function of the solar multiple. *Sol. Energy* **2009**, *83*, 679–689. [CrossRef]
5. Montes, M.J.; Abánades, A.; Martínez-Val, J.M.; Valdés, M. Solar multiple optimization for a solar-only thermal power plant, using oil as heat transfer fluid in the parabolic trough collectors. *Sol. Energy* **2009**, *83*, 2165–2176. [CrossRef]
6. Desai, N.B.; Bandyopadhyay, S. Optimization of concentrating solar thermal power plant based on parabolic trough collector. *J. Clean. Prod.* **2015**, *89*, 262–271. [CrossRef]
7. Odeh, S.D.; Morrison, G.L.; Behnia, M. Modelling of parabolic trough direct steam generation solar collectors. *Sol. Energy* **1998**, *62*, 395–406. [CrossRef]
8. Post, A.D.; King, B.V.; Kisi, E.H. Computational model and optimisation of a vacuum diode thermionic generator for application in concentrating solar thermal power. *Appl. Therm. Eng.* **2017**, *117*, 245–253.
9. Bishoyi, D.; Sudhakar, K. Modeling and performance simulation of 100 MW PTC based solar thermal power plant in Udaipur India. *Case Stud. Therm. Eng.* **2017**, *10*, 216–226.
10. Ruegamer, T.; Kamp, H.; Kuckelkorn, T.; Schiel, W.; Weinrebe, G.; Nava, P.; Riffelmann, K.; Richert, T. Molten salt for parabolic trough applications: System simulation and scale effects. *Energy Procedia* **2014**, *49*, 1523–1532. [CrossRef]
11. Lenert, A.; Wang, E.N. Optimization of nanofluid volumetric receivers for solar thermal energy conversion. *Sol. Energy* **2012**, *86*, 253–265. [CrossRef]
12. Ramteen, S.; Denholm, P. The value of concentrating solar power and thermal energy storage. *IEEE Trans. Sustain. Energy* **2010**, *1*, 173–183.
13. Avila-Marin, A.L.; Fernandez-Reche, J.; Tellez, F.M. Evaluation of the potential of central receiver solar power plants: Configuration, optimization and trends. *Appl. Energy* **2013**, *112*, 274–288. [CrossRef]
14. Gur, M.; Epstein, M. A novel power block for CSP systems. *Sol. Energy* **2010**, *84*, 1761–1771.
15. Sait, H.H.; Martinez-Val, J.M.; Abbas, R.; Munoz-Anton, J. Fresnel-based modular solar fields for performance/cost optimization in solar thermal power plants: A comparison with parabolic trough collectors. *Appl. Energy* **2015**, *141*, 175–189. [CrossRef]
16. Desai, N.B.; Bandyopadhyay, S. Integration of parabolic trough and linear Fresnel collectors for optimum design of concentrating solar thermal power plant. *Clean Technol. Environ. Policy* **2015**, *17*, 1945–1961. [CrossRef]
17. Boukelia, T.E.; Arslan, O.; Mecibah, M.S. ANN-based optimization of a parabolic trough solar thermal power plant. *Appl. Therm. Eng.* **2016**, *107*, 1210–1218. [CrossRef]
18. Cabello, J.M.; Cejudo, J.M.; Luque, M.; Ruiz, F.; Deb, K.; Tewari, R. Optimization of the size of a solar thermal electricity plant by means of genetic algorithms. *Renew. Energy* **2011**, *36*, 3146–3153. [CrossRef]
19. Dowling, A.; Zheng, T.; Zavala, V. Economic assessment of concentrated solar power technologies: A review. *Renew. Sustain. Energy Rev.* **2017**, *72*, 1019–1032. [CrossRef]
20. Dominquez-Munoz, F.; Cejuda-Lopez, J.; Carrillo-Andres, A.; Ruiv, C. Design of solar thermal systems under uncertainty. *Energy Build.* **2012**, *47*, 474–484. [CrossRef]

21. Jain, A.; Tuyet, V.; Mehta, R.; Mittala, S. Optimizing the Cost and Performance of Parabolic Trough Solar Plants with Thermal Energy Storage in India. *Environ. Prog. Sustain. Energy* **2013**, *32*, 824–829. [CrossRef]
22. Meybodi, M.; Beath, A. Impact of cost uncertainties and solar data variations on the economics of central receiver solar power plants: An Australian case study. *Renew. Energy* **2016**, *93*, 510–524. [CrossRef]
23. Hanel, M.; Escobar, R. Influence of solar energy resource assessment uncertainty in the levelized electricity cost of concentrated solar power plants in Chile. *Renew. Energy* **2013**, *49*, 96–100. [CrossRef]
24. Ho, C.; Kolb, G. Incorporating Uncertainty into Probabilistic Performance Models of Concentrating Solar Power Plants. *J. Sol. Energy Eng.* **2010**, *132*, 031012. [CrossRef]
25. Pousinho, H.M.I.; Contreras, J.; Pinson, P.; Mendes, V.M.F. Robust optimisation for self-scheduling and bidding strategies of hybrid CSP—Fossil power plants. *Int. J. Electr. Power Energy Syst.* **2015**, *67*, 639–650. [CrossRef]
26. Poland, J.; Stadler, K. Stochastic Optimal Planning of Solar Thermal Power. In Proceedings of the 2014 IEEE Conference on Control Applications (CCA) Part of 2014 IEEE Multi-Conference on Systems and Control, Antibes, France, 8–10 October 2014.
27. Dominguez, R.; Conejo, B. Optimal offering strategy for a concentrating solar power plant. *Appl. Energy* **2012**, *98*, 316–325. [CrossRef]
28. Guédeza, R.; Spellinga, J.; Laumerta, B. Thermoeconomic Optimization of Solar Thermal Power Plants with Storage in High-Penetration Renewable Electricity Markets. *Energy Procedia* **2014**, *57*, 541–550. [CrossRef]
29. Li, Q.; Wang, J.; Zhang, Y.; Fan, Y.; Bao, G.; Wang, X. Multi-Period Generation Expansion Planning for Sustainable Power Systems to Maximize the Utilization of Renewable Energy Source. *Sustainability* **2020**, *12*, 1083. [CrossRef]
30. Sahin, K.; Diwekar, U. Better Optimization of Nonlinear Uncertain Systems (BONUS): A New Algorithm for Stochastic Programming Using Reweighting through Kernel Density Estimation. *Ann. Oper. Res.* **2004**, *132*, 47–68. [CrossRef]
31. SAM. Available online: https://sam.nrel.gov/sites/sam.nrel.gov/files/content/documents/pdf/sam-help.pdf (accessed on 16 June 2020).
32. Mubarak, R.; Hofmann, M.; Riechelmann, S.; Seckmeyer, G. Comparison of modelled and measured tilted solar irradiance for photovoltaic applications. *Energies* **2017**, *10*, 1688. [CrossRef]
33. Ceci1, M.; Corizzol, R.; Malerba, D.; Rashkovska, A. Spatial autocorrelation and entropy for renewable energy forecasting. *Data Min. Knowl. Discov.* **2019**, *33*, 698–729. [CrossRef]
34. Diwekar, U.M. *Introduction to Applied Optimization*; Springer: New York, NY, USA, 2008.
35. Diwekar, U.; David, A. *BONUS Algorithm for Large Scale Stochastic Nonlinear Programing Problems*; Springer: Berlin/Heidelberg, Germany, 2015.
36. Charnes, A.; Cooper, W.W. Chance-constrained programming. *Manag. Sci.* **1959**, *5*, 73–79. [CrossRef]
37. Ozturk, U.; Mazumdar, M.; Norman, B. A solution to the stochastic unit commitment problem using chance constrained programming. *IEEE Trans. Power Syst.* **2004**, *19*, 1589–1598. [CrossRef]
38. Wei, J.; Zhanga, Y.; Wanga, J.; Caob, X.; Khana, M.A. Multi-Period Planning of Multi-Energy Microgrid with Multi-Type Uncertainties Using Chance Constrained Information Gap Decision Method. *Appl. Energy* **2020**, *260*, 114188. [CrossRef]
39. Chowdhury, N.; Pilo, F.; Pisano, G. Optimal Energy Storage System Positioning and Sizing with Robust Optimizatio. *Energies* **2020**, *13*, 512. [CrossRef]
40. Birge, J.R.; Louveaux, F. *Introduction to Stochastic Programming*; Springer: New York, NY, USA, 1997.
41. Ruszczynski, A. A regularized decomposition for minimizing a sum of polyhedral functions. *Math. Program.* **1986**, *35*, 309. [CrossRef]
42. Rockafellar, R.T.; Wets, R.J.-B. Scenarios and policy aggregation in optimization under uncertainty. *Math. Oper. Res.* **1991**, *16*, 119. [CrossRef]
43. Dantzig, G.B.; Infanger, G. Large scale stochastic linear programs—Importance sampling and Bender decomposition. In *Computational and Applied Mathematics*; Brezinski, C., Kulisch, U., Eds.; Stanford University: Stanford, CA, USA, 1991; pp. 111–120.
44. Higle, J.L.; Sen, S. Stochastic decomposition: An algorithm for two-stage linear programs with recourse. Math. *Oper. Res.* **1991**, *16*, 650–669. [CrossRef]
45. Diwekar, U.; Ulas, S. Sampling Techniques. In *Kirk-Othmer Encyclopedia of 358 Chemical Technology*, Online ed.; John and Wiley and Sons: Hoboken, NJ, USA, 2007; Volume 26, p. 998.

46. Diwekar, U.M.; Kalagnanam, J.R. An efficient sampling technique for optimization under uncertainty. *AIChE J.* **1997**, *43*, 440. [CrossRef]
47. Eia. Annual Energy Outlook 2015. Available online: https://www.eia.gov/outlooks/aeo/pdf/0383(2015).pdf (accessed on 16 June 2020).
48. Eia. Annual Energy Outlook 2019. Available online: https://www.eia.gov/outlooks/aeo/pdf/aeo2019.pdf (accessed on 16 June 2020).